Analysis of a Lys-specific serine endopeptidase secreted via the type IX secretion system in *Porphyromonas gingivalis*

Minako Nonaka, Mikio Shoji, Tomoko Kadowaki*, Keiko Sato, Hideharu Yukitake, Mariko Naito, and Koji Nakayama

Division of Microbiology and Oral Infection, Department of Molecular Microbiology and Immunology, Nagasaki University Graduate School of Biomedical Sciences, Nagasaki, Japan

*Present address: University Research Administration Office, Nagasaki University, Nagasaki, Japan

Correspondence: Koji Nakayama, Division of Microbiology and Oral Infection, Department of Molecular Microbiology and Immunology, Nagasaki University Graduate School of Biomedical Sciences, Nagasaki 852-8588, Japan. Tel: +81 95 7648; Fax: +81 95 819 7650; E-mail: knak@nagasaki-u.ac.jp

Keywords: endopeptidase, protein secretion system, periodontal disease, oral anaerobic bacterium

Running title: T9SS-secreted Lys-specific serine endopeptidase

Abstract

Porphyromonas gingivalis, a significant causative agent of adult periodontitis, possesses a novel secretion system called the type IX secretion system (T9SS). A number of virulence factors, such as Arg-gingipain (Rgp), are translocated onto the cell surface and into the extracellular milieu via the T9SS. In this study, we found that the PGN_1416 90 to 120 kDa diffuse protein bands were located in the outer membrane fraction and that the presence of the bands was dependent on genes involved in the T9SS and the formation of anionic lipopolysaccharide (A-LPS). These data strongly suggest that the PGN_1416 protein is secreted by the T9SS and anchored onto the cell surface by binding to A-LPS. Enzymatic analysis using outer membrane fractions suggested that the PGN_1416 protein has a Lys-specific serine endopeptidase activity and that its activation requires processing by Rgp. Homologues of the gene encoding PGN_1416, which is referred to as *pepK*, were found in bacteria belonging to the phyla *Bacteroidetes* and *Proteobacteria*, while homologues encoding the C-terminal domain, which is essential for T9SS-mediated secretion, and the catalytic domain were only observed in bacteria belonging to the *Bacteroidetes* phylum.

Introduction

The periodontal diseases periodontitis and gingivitis, which are defined as inflammatory diseases of the periodontal tissues, are induced by bacterial infection. *Porphyromonas gingivalis,* a Gram-negative anaerobic bacterium, is closely associated with the aetiology of periodontitis; the microorganism is detected in 85.7% of patients suffering from the disease (Yang *et al*., 2004). *P. gingivalis* possesses a number of virulence factors, such as proteinases, haemagglutinins, lipopolysaccharide (LPS), capsule and fimbriae (Nakayama *et al*., 1996; Lamont & Jenkinson, 1998).

The majority of the proteolytic activity of the culture supernatants and the bacterial surfaces is derived from gingipains, which are categorised into two major classes of extracellular cysteine proteinases specific for Arg-X and Lys-X peptide bonds [Arg-gingipains (Rgps) and Lys-gingipain (Kgp)] (Curtis *et al*., 1999). Rgps are encoded by *rgpA* and *rgpB*, and Kgp is encoded by *kgp* (Curtis *et al*., 1999). The physiological functions of gingipains involve metabolism and virulence, such as acquisition of energy sources, degradation of host defence proteins and processing of bacterial proteins, including fimbrial subunits (Kadowaki *et al*., 2000).

We previously found that the gene products of *rgpA*, *rgpB* and *kgp* were translocated across the outer membrane by the Por secretion system, which is now referred to as the type IX secretion system (T9SS) and which involves the *porK*, *porL*, *porM*, *porN*, *porP*, *porQ*, *porT*, *porU*, *porV*, *porW* and *sov* gene products (Sato *et al*., 2010; McBride & Zhu, 2013). Homologues of these genes are found in a number of bacteria belonging to the phylum *Bacteroidetes* and associated with *Bacteroidetes* gliding motility (McBride & Zhu, 2013; Nakane *et al*., 2013). Comparison of the protein profiles from

particle-free culture supernatants between T9SS-proficient and T9SS-deficient strains revealed that 10 proteins, including the PGN_1416 protein, were detected only in the culture supernatant derived from the T9SS-proficient strain (Sato *et al*., 2013). The PGN_1416 protein contains the C-terminal domain (CTD) that is commonly observed in proteins secreted via the T9SS (Sato *et al*., 2013). These findings suggest that the PGN_1416 protein is secreted by the T9SS. The PGN_1416 protein is predicted to be a lysyl endopeptidase based on a bioinformatic resource analysis (Kyoto Encyclopedia of Genes and Genomes; KEGG). The gene encoding the PGN_1416 protein was tentatively designated *pepK* (gene for Lys (K)-specific endopeptidase) in this study. However, the biological and biochemical properties of the PGN_1416 protein in *P. gingivalis* are unknown.

In this study, we examined various *P. gingivalis* strains for the presence of PGN_1416 proteins using anti-PGN_1416 antiserum. In addition, we constructed PGN_1416-deficient mutants and performed biological and biochemical analyses comparing these mutants with their parent strains. The results presented here strongly suggest that the PGN_1416 protein is secreted via the T9SS and is a serine endopeptidase with the ability to digest a Lys-X peptide bond.

Materials and Methods

Bacterial strains and plasmids

The bacterial strains and plasmids used in this study are listed in Tables S1 and S2, respectively.

Media and bacterial growth conditions

Media and conditions for growth of *P. gingivalis* and *Escherichia coli* strains used in this study have been previously described (Shoji *et al.*, 2013).

Chemicals

The proteinase inhibitors *N*α-*p*-tosyl-L-lysine chloromethyl ketone (TLCK) and EDTA-Na_2 were purchased from Wako. Other inhibitors and synthetic substrates were obtained from the Peptide Institute.

Polyclonal antibody

To prepare recombinant PGN_1416 protein for use as an antigen, the DNA fragment between bases 1,381 and 2,580, encoding 400 amino acids, was amplified from the PGN_1416-encoding gene of *P. gingivalis* ATCC 33277 with primers 1416DOFOR and 1416DOREV (Table S3). The resulting fragment was inserted into the *Nco*I-*Hin*dIII site of plasmid pET32b, generating pKD601. *E. coli* BL21(DE3) cells harbouring pKD601 were grown in LB broth and induced with isopropyl β-D-thiogalactoside at a final concentration of 1 mM, followed by incubation for 2 h to overproduce the recombinant protein. The induced recombinant protein was purified using a

Ni-nitrilotriacetic acid purification system (Clontech). To obtain antiserum against the PGN_1416 protein, mice were immunised with 10 μg of recombinant protein in conjunction with Freund's incomplete adjuvant (Sigma). The injections were performed at 2-week intervals. The blood was collected after four injections. Mouse polyclonal antiserum was harvested from the blood by centrifugation at 3,000 x *g* for 10 min at 4°C after an overnight incubation at 4°C and stored at -20°C until the immunoblot analyses.

Construction of bacterial strains

The DNA regions upstream and downstream of a gene were PCR amplified from the chromosomal DNA of *P. gingivalis* ATCC 33277 using primer pairs N1416-UR and N1416-UR and N1416-DF and N1416-DR, respectively (U indicates upstream, F indicates forward, D indicates downstream, and R indicates reverse). The primers used in this study are listed in Table S3. The amplified upstream DNA fragment was digested with *Hin*dIII and *Bam*HI. The amplified downstream DNA was digested with *Not*I and *Bam*HI. Both digested products were ligated together with pBluescript II SK(−), which had been digested with *Hin*dIII and *Not*I. The 1.5-kb *Bam*HI *ermF* DNA fragment was inserted into the *Bam*HI site of the resulting plasmids to yield pKD600 for mutagenesis. The plasmid was digested with *Not*I and introduced into *P. gingivalis* ATCC 33277 and KDP129 (*kgp*::Cm^r) by electroporation to produce KDP600 (*pepK*::Em^r) and KDP601 (*kgp*::Cm^r *pepK*::Em^r), respectively.

Sample preparation

Membrane fraction. *P. gingivalis* grown to mid-log phase was subjected to the

following fractionation as previously described (Murakami *et al*., 2002). Briefly, the cells were harvested by centrifugation at 10,000 x *g* for 20 min, washed twice with 10 mM HEPES-NaOH buffer (pH 7.4) containing 150 mM NaCl, suspended in 10 mM HEPES buffer (pH 7.4) with 10 μM E-64 and disrupted in a French pressure cell at 100 MPa. Unbroken cells and large debris were removed by centrifugation at 1,000 x *g* for 10 min, and the supernatants (whole-cell lysates) were subjected to ultracentrifugation at 100,000 x *g* for 1 h. The precipitates were suspended in 10 mM HEPES buffer (pH 7.4) containing 20 mM $MgCl_2$ supplemented with Triton X-100 at a final concentration of 1% and mixed gently at room temperature (RT) for 30 min. The solution was subjected to ultracentrifugation at 100,000 x *g* for 1 h to yield the bacterial outer membrane fraction as the precipitate.

Sucrose density gradient centrifugation. Sucrose density gradient centrifugation was performed as previously described (Shoji *et al*., 2013).

Supernatant fractions. A vesicle fraction (v.f.) was obtained by ultracentrifugation of the supernatants at 100,000 x *g* for 1 h at 4°C. Proteins in the supernatant fraction without vesicles were precipitated with trichloroacetic acid and used for SDS–PAGE and immunoblot analysis as a particle free fraction (p.f.f.).

Gel electrophoresis and immunoblot analysis

SDS-PAGE and immunoblot analysis were performed as previously described (Shoji *et al.* 2010, 2011).

Dot blot analysis

Dot blot analysis was performed as described previously (Shoji *et al*., 2011), with some

158 modifications. Briefly, *P. gingivalis* cells that had fully grown in enriched BHI
159 medium were harvested, washed with PBS and suspended with PBS. The washed cells
160 were adjusted to an OD595 of 1.0. Three microliters of the adjusted cells was blotted
161 directly onto a nitrocellulose membrane and left to dry.
162
163 **Fluorometric assay**
164 A Triton X-100-insoluble outer membrane fraction from each strain was used for all
165 enzymatic assays. Sample protein concentration was measured by the Bradford method
166 (Bio-Rad) with bovine serum albumin as the standard. The proteolytic activities were
167 determined with the synthetic substrates Boc-Val-Leu-Lys-MCA,
168 Boc-Phe-Ser-Arg-MCA, Suc-Ala-Ala-Pro-Phe-MCA, Suc-Gly-Pro-MCA and
169 Suc(OMe)-Ala-Ala-Pro-Val-MCA. The reaction mixture (450 μl) contained equal
170 protein amounts from the outer membrane fractions of ATCC 33277, KDP129, KDP601
171 and KDP981 and 10 μM of each synthetic substrate in 150 mM Tris-HCl (pH 9.2). For
172 the fluorometric enzyme assays, the reaction mixture without the synthetic substrates
173 was incubated at 37°C for 5 min, placed on ice and then, the synthetic substrates were
174 added to the reaction mixture. After incubation at 40°C for 10 min, the reaction was
175 terminated by the addition of 45% acetic acid, and the released MCA was then
176 measured at 465 nm (excitation at 365 nm) on a fluorescence spectrophotometer.
177

Results

Immunoblot analysis of various *P. gingivalis* strains with anti-PGN_1416 antiserum

Cell lysates of *P. gingivalis* ATCC 33277, W83, TDC60, TDC117, TDC275, GAI7802, SU63 and HG66 were subjected to immunoblot analysis with anti-PGN_1416 antiserum. As shown in Figure 1a, all of the strains except HG66 exhibited diffuse protein bands with molecular masses of 50 to 120 kDa, and all the strains, including HG66, had a discrete protein band with a molecular mass of 95 kDa. We constructed a PGN_1416-deficient (*pepK*) mutant, which showed no reactivity to anti-PGN_1416 antiserum (Fig. 1b), verifying that the reactive protein bands were derived from PGN_1416. The results suggest that the PGN_1416 protein is generally produced in *P. gingivalis*.

Previous studies indicated that T9SS-dependent secretion proteins, such as gingipains and HBP35, are located at the outer membrane by attaching to A-LPS, which results in the formation of diffuse protein bands (Nakayama *et al*., 1995; Shoji *et al*., 2010). To determine whether the generation of the diffuse PGN_1416 protein bands is dependent on T9SS and A-LPS, immunoblot analysis of T9SS-deficient and A-LPS-deficient mutants with anti-PGN_1416 antiserum was performed (Fig. 1b and c).

We previously reported that *P. gingivalis porK* (PGN_1676), *porL* (PGN_1675), *porM* (PGN_1674), *porN* (PGN_1673), *porP* (PGN_1677), *porQ* (PGN_0645), *porT* (PGN_0778), *porU* (PGN_0022), *porV* (PGN_0023), *porW* (PGN_1877) and *sov* (PGN_0832) mutants were defective in the T9SS (Sato *et al*., 2010; Shoji *et al*., 2011). These mutants showed no diffuse PGN_1416 protein bands, suggesting that the PGN_1416 protein is secreted via T9SS (Fig. 1b).

Next, we determined whether the diffuse PGN_1416 protein bands were present in

A-LPS-deficient mutants. We used PGN_0242, PGN_0663, PGN_1056 (VimA), PGN_1236 (PorR), PGN_1242 (Wzy), PGN_1251 (GtfB), PGN_1255 (Rfa), PGN_1302 (WaaI) and PGN_2005 (WzzP) mutants as A-LPS-deficient mutants. None of the A-LPS-deficient mutants examined had the diffuse protein bands, which suggests that the diffuse PGN_1416 protein bands were generated by attaching to A-LPS (Fig. 1c).

Subcellular location of the various PGN_1416 protein forms

Subcellular fractionation analysis revealed that the diffuse 50-120 kDa protein bands were located in the total membrane fraction (Fig. 2a). A 46-kDa protein reactive with anti-PGN_1416 was detected in the cytoplasmic/periplasmic and total membrane fractions. Next, the total membrane fraction was separated into inner and outer membrane fractions using sucrose density gradient centrifugation (Fig. 2b). The inner and outer membrane fractions were determined by the presence of the highest NADH-dependent ferricyanide reductase activity and LPS, respectively. The 95-kDa protein was found in the inner membrane fraction, whereas the diffuse protein bands were in the outer membrane fraction, which suggests that the PGN_1416 protein was located at the outer membrane as a diffuse form with molecular masses of 90-120 kDa (Fig. 2b). The diffuse form of the PGN_1416 protein was also observed in the vesicle fraction, whereas the PGN_1416 protein with a molecular mass of 65 kDa was located in the particle-free fraction of the culture supernatants (Fig. 2c).

T9SS-dependent localization of the PGN_1416 protein on the cell surface

Dot blot analysis revealed that the PGN_1416 protein was detected on the cell surface

of the wild-type strain, whereas it was not detected on that of the *porK* or *porT* mutant (Fig. 2d).

Endopeptidase activity of a Triton X-100 insoluble fraction of the total membrane fraction

Bioinformatic resource analysis (Kyoto Encyclopedia of Genes and Genomes KEGG) suggested that the PGN_1416 protein is a lysyl endopeptidase. We constructed a PGN_1416-deficient (*pepK*) mutant from the *kgp* strain to exclude the enzymatic activity derived from Kgp. We then compared endopeptidase activities of Triton X-100-insoluble fractions of the total membrane fractions from the *kgp pepK* mutant and *kgp* parent strain because the PGN_1416 protein was located at the outer membrane by attaching to A-LPS. Using the synthetic substrate Boc-Val-Leu-Lys-MCA, lysyl endopeptidase activity was detected in the Triton X-100-insoluble fraction of the *kgp* strain in a concentration-dependent manner, whereas the activity of the *kgp pepK* mutant was significantly attenuated and not dependent on a protein concentration (Fig. 3a). Conversely, the ability to digest an Arg-X peptide bond was detected in both the *kgp* and *kgp pepK* mutants (Fig. 3b). The ability to digest Pro-X, Val-X or Phe-X peptide bond was not detected (data not shown). These results strongly suggest that *P. gingivalis* possess lysyl endopeptidase activity other than Kgp at the outer membrane and that the Lys-specific activity was derived from the *pepK* gene. Comparison of Lys-specific activities of the Triton X-100-insoluble fractions of the wild type, *kgp* and *kgp pepK* strains suggested that Lys-specific activity of PepK per cell was approximately one fortieth of that of Kgp per cell (data not shown).

We examined the effects of various proteinase inhibitors on the endopeptidase

activity specific for the Lys-X peptide bond (Table 1). The Lys-specific activity disappeared completely in the presence of leupeptin and antipain, which are serine proteinase inhibitors. Tosyllysine chloromethyl ketone (TLCK) and chymostatin, which are also serine proteinase inhibitors, significantly suppressed the activity. Neither ethylene diaminetetraacetic acid (EDTA) as a metalloproteinase inhibitor nor pepstatin as an aspartic acid proteinase inhibitor inhibited the activity. Taken together, these results indicate that the activity detected in the outer membrane fraction is due to the presence of a Lys-specific serine endopeptidase.

Involvement of Rgp in activation of the Lys-specific serine endopeptidase

Interestingly, a Triton X-100-insoluble fraction of the total membrane fraction from the *kgp rgpA rgpB* mutant showed no Lys-specific activity, whereas that of the *kgp* mutant did show Lys-specific activity (Fig. 3c). To investigate whether the Rgp proteinase influences activation of the Lys-specific serine endopeptidase, the *kgp rgpA rgpB* and *kgp pepK* mutants were co-cultured, and the Lys-specific activity of the Triton X-100-insoluble fraction of the total membrane fraction from the co-culture was determined. The Lys-specific activity of the co-culture was dependent on protein concentration and was clearly higher than that of the *kgp pepK* mutant. The activity was approximately 60-80% of that of the *kgp* mutant (Fig. 3c).

To investigate the effects of gingipains on the molecular masses of various forms of PepK, various gingipain-deficient mutants were subjected to immunoblot analysis with anti-PepK antiserum (Fig. 4a and b). The diffuse protein bands in the gingipain-null mutant (*kgp rgpA rgpB*) migrated at higher molecular masses than that of the wild-type. In connection with the change of molecular masses of diffuse protein bands, the 46-kDa

PepK protein band, which was observed in the wild-type, *kgp, rgpA, rgpB, kgp rgpA* and *kgp rgpB* mutants, was not observed in the *rgpA rgpB* and *kgp rgpA rgpB* strains. Next, the co-culture of the *kgp rgpA rgpB* mutant with the *kgp pepK* mutant was subjected to immunoblot analysis with anti-PepK (Fig. 4c). The diffuse PepK protein bands of the co-culture had lower molecular masses than those of the *kgp rgpA rgpB* mutant, and the 46-kDa PepK protein band appeared in the co-culture. These results suggest that Rgp processes and activates the PepK protein.

283 **Discussion**

284

285 Our recent study (Sato *et al*., 2013) found that the PGN_1416 protein is detected in the
286 particle-free culture supernatant of a T9SS-proficient strain (*kgp rgpA rgpB*) but not in
287 the particle-free culture supernatant of a T9SS-deficient strain (*kgp rgpA rgpB porK*).
288 Additional analysis revealed that the PGN_1416 protein possesses a CTD-like sequence
289 at the C-terminus. Several lines of evidence indicate that PepK is secreted via the
290 T9SS. First, the 50-120 kDa diffuse PepK proteins were located at the outer
291 membrane. Second, A-LPS-deficient strains showed no diffuse protein bands
292 immunoreactive to anti-PepK. Third, the presence of the 50-120 kDa diffuse PepK
293 proteins was dependent on T9SS-related genes.

294 According to a bioinformatic database analysis, PepK may be a lysyl endopeptidase.
295 In *P. gingivalis*, the Lys-specific endopeptidase with the highest activity is Kgp.
296 Therefore, in this study, we compared Lys-specific endopeptidase of the *kgp pepK*
297 mutant strain with that of the parent *kgp* mutant strain and found Lys-specific
298 endopeptidase activity in the Triton X-100-insoluble membrane fraction of the *kgp*
299 strain but not in the *kgp pepK* strain. The PepK endopeptidase activity was sensitive to
300 serine proteinase inhibitors. Chohnan *et al*. (2004) reported lysyl endopeptidases from
301 *Lysobacter* sp. strain IB-9374. The putative catalytic triad of the *Lysobacter*
302 peptidases was conserved in the amino acid sequence of PepK (Fig. 5a). These results
303 strongly suggest that PepK is a Lys-specific serine endopeptidase.

304 Interestingly, catalytic activity of PepK was not detected in the outer membrane
305 fraction of the *kgp rgpA rgpB* mutant, and the activity was recovered by co-culture with
306 the *kgp pepK* mutant, suggesting that PepK is activated by Rgp. The results obtained

using immunoblot analysis were consistent with the co-culture activity analysis. Rgp-processed proteins have been previously reported. Fimbrillins, such as FimA and Mfa1, are processed on the cell surface by Rgp, resulting in the assembly of Fim and Mfa fimbriae, respectively (Nakayama *et al*., 1996). Nelson *et al*. (1999) suggested that the pro-form of periodontain, which is capable of inactivating human serpin, is processed by both Rgp and Kgp. Gingipains were also found to cleave and process the products encoded by *rgpA, rgpB, kgp, hagA* and *ragA* (Kadowaki *et al*. 1998; Murakami *et. al*., 2002; Veith *et al*., 2002). These proteins, including PepK, are activated by gingipains, but gingipain-sensitive ligand A (GslA), which is able to induce cell signalling, is degraded and inactivated by gingipains (Haruyama *et al*., 2009). All of the gingipain-processed *P. gingivalis* proteins found thus far are located on the cell surface.

Genes homologous to *pepK* are mainly found in bacteria in genera belonging to the phylum *Bacteroidetes*, such as *Porphyromonas, Parabacteroides*, and *Tannerella*. Proteins encoded by these homologous genes, which are composed of more than 800 amino acid residues, appear to have a CTD at the C-terminus (Fig. 5b). Interestingly, amino acid sequences homologous to the catalytic domain of PepK are found not only in the CTD-containing proteins in *Bacteroidetes* bacteria but also in the proteins of bacteria in genera belonging to the phylum *Proteobacteria*, such as *Acidovorax, Pseudomonas, Lysobacter* and *Xanthomonas* (Fig. 5a). These *Proteobacteria* proteins are generally smaller than the PepK homologues found in *Bacteroidetes* bacteria, especially in the C-terminal region. This analysis suggests that a prototype of the PepK homologues in *Bacteroidetes* bacteria was likely generated by addition of a C-terminal region containing the CTD sequence to a catalytic domain with a propeptide

region.

The *pepK* mutant showed no changes in Rgp and Kgp activity compared with the wild-type parent strain, formed black-pigmented colonies on the blood agar and possessed wild-type levels of fimbriae on the cell (data not shown). These findings indicate that PepK has no effect on gingipain activities, colonial pigmentation or the formation of fimbriae. However, the wide distribution of *pepK* homologues beyond the phylum *Bacteroidetes* may be associated with the virulence potential of each bacterium, although further studies are needed to determine if the presence of *pepK* is influential in the pathogenesis of *P. gingivalis*.

Acknowledgements

This work was supported by Grants-in-Aid for Scientific Research (to K.N.) from the Ministry of Education, Culture, Sports, Science, and Technology of Japan.

346 **References**

347

348 Chohnan S, Shiraki K, Yokota K, Ohshima M, Kuroiwa N, Ahmed K, Masaki T &
349 Sakiyama F (2004) A second lysine-specific serine protease from *Lysobacter* sp.
350 Strain IB-9374. *J Bacteriol* **186**: 5093–5100.

351 Curtis MA, Kuramitsu HK, Lantz M, Macrina FL, Nakayama K, Potempa J, Reynolds
352 EC & Aduse-Opoku J (1999) Molecular genetics and nomenclature of proteases of
353 *Porphyromonas gingivalis*. *J Periodontal Res* **34**: 464-472.

354 Futai M (1974) Orientation of membrane vesicles from *Escherichia coli* prepared by
355 different procedures. *J Membr Biol* **15**: 15-28.

356 Haruyama K, Yoshimura A, Naito M, Kishimoto M, Shoji,M, Abiko Y, Hara Y &
357 Nakayama K (2009) Identification of a gingipain-sensitive surface ligand of
358 *Porphyromonas gingivalis* that induces Toll-like receptor 2- and 4-independent
359 NF-κB activation in CHO cells. *Infect Immun* **77**: 4414–4420.

360 Kadowaki T, Nakayama K, Yoshimura F, Okamoto K, Abe N & Yamamoto K (1998)
361 Arg-gingipain acts as a major processing enzyme for various cell surface proteins in
362 *Porphyromonas gingivalis*. *J Biol Chem* **273**: 29072-29076.

363 Kadowaki T, Nakayama K, Okamoto K, Abe N, Baba A, Shi Y, Ratnayake DB &
364 Yamamoto K (2000) *Porphyromonas gingivalis* proteinases as virulence
365 determinants in progression of periodontal diseases. *J. Biochem* **128:** 153-159.

366 Lamont RJ & Jenkinson HF (1998) Life below the gum line: pathogenic mechanisms of
367 *Porphyromonas gingivalis*. *Microbiol Mol Biol Rev* **62**: 1244–1263.

368 McBride MJ & Zhu Y (2013) Gliding motility and Por secretion system genes are
369 widespread among members of the phylum *Bacteroidetes*. *J. Bacteriol* **195**: 270-278.

370 Murakami Y, Imai M, Nakamura H & Yoshimura F (2002) Separation of the outer
371 membrane and identification of major outer membrane proteins from
372 *Porphyromonas gingivalis*. *Eur J Oral Sci* **110**: 157–162.
373 Nakane D, Sato K, Wada H, McBride MJ & Nakayama K (2013) Helical flow of
374 surface protein required for bacterial gliding motility. *P Natl Acad Sci USA* **110**:
375 11145-11150.
376 Nakayama K, Kadowaki T, Okamoto K & Yamamoto K (1995) Construction and
377 characterization of arginine-specific cysteine proteinase (Arg-gingipain)-deficient
378 mutants of *Porphyromonas gingivalis*. Evidence for significant contribution of
379 Arg-gingipain to virulence. *J Biol Chem* **270**: 23619–23626.
380 Nakayama K, Yoshimura F, Kadowaki T & Yamamoto K (1996) Involvement of
381 Arginine-Specific Cysteine Proteinase (Arg-Gingipain) in Fimbriation of
382 *Porphyromonas gingivalis*. *J Bacteriol* **178**: 2818–2824.
383 Nelson D, Potempa J, Kordula T & Travis J (1999) Purification and characterization of
384 a novel cysteine proteinase (Periodontain) from *Porphyromonas gingivalis*. *J Biol*
385 *Chem* **274**: 12245–12251.
386 Sato K, Sakai E, Veith PD, Shoji M, Kikuchi Y, Yukitake H, Ohara N, Naito M,
387 Okamoto K, Reynolds EC & Nakayama K (2005) Identification of a new
388 membrane-associated protein that influences transport/maturation of gingipains and
389 adhesins of *Porphyromonas gingivalis*. *J Biol Chem* **280**: 8668-8677.
390 Sato K, Kido N, Murakami Y, Hoover CI, Nakayama K & Yoshimura F (2009)
391 Lipopolysaccharide biosynthesis-related genes are required for colony pigmentation
392 of *Porphyromonas gingivalis*. *Microbiology* **155**: 1282–1293.
393

394 Sato K, Naito M, Yukitake H, Hirakawa H, Shoji M, McBride MJ, Rhodes RG &
395 Nakayama K (2010) A protein secretion system linked to bacteroidete gliding
396 motility and pathogenesis. *P Natl Acad Sci USA* **107**: 276–281.
397 Sato K, Yukitake H, Narita Y, Shoji M, Naito M & Nakayama K (2013) Identification of
398 *Pophyrmonas gingivalis* proteins secreted by the Por secretion system. *FEMS*
399 *Microbiol Lett* **338**: 68–76.
400 Shi Y, Ratnayake DB, Okamoto K, Abe N, Yamamoto K & Nakayama K (1999) Genetic
401 analyses of proteolysis, hemoglogin binding, and hemagglutination of
402 *Porphyromonas gingivalis*. Construction of mutants with a combination of *rgpA*,
403 *rgpB*, *kgp*, and *hagA*. *J Biol Chem* **274**: 17955–17960.
404 Shoji M, Ratnayake DB, Shi Y, Kadowaki T, Yamamoto K, Yoshimura F, Akamine A,
405 Curtis MA & Nakayama K (2002) Construction and characterization of a
406 nonpigmented mutant of *Porphyromonas gingivalis*: cell surface polysaccharide as
407 an anchorage for gingipains. *Microbiology* **148**: 1183–1191.
408 Shoji M, Shibata Y, Shiroza T, Yukitake H, Peng B, Chen YY, Sato K, Naito M, Abiko Y,
409 Reynolds EC & Nakayama K (2010) Characterization of hemin-binding protein 35
410 (HBP35) in *Porphyromonas gingivalis*: its cellular distribution, thioredoxin activity
411 and role in heme utilization. *BMC Microbiol* **10**: 152.
412 Shoji M, Sato K, Yukitake H, Kondo Y, Narita Y, Kadowaki T, Naito M & Nakayama K
413 (2011) Por secretion system-dependent secretion and glycosylation of
414 *Porphyromonas gingivalis* hemin-binding protein 35. *PLoS ONE* **6**: e21372.
415 Shoji M, Yukitake H, Sato K, Shibata Y, Naito M, Aduse-Opoku J, Abiko Y, Curtis MA
416 & Nakayama K (2013) Identification of an O-antigen chain length regulator, WzzP,
417 in *Porphyromonas gingivalis*. *MicrobiologyOpen* **2**: 383–401.

418 Simon R, Priefer U & Puhler A (1983) A broad host range mobilization system for in
419 vivo genetic engineering: transposon mutagenesis in Gram negative bacteria.
420 *Biotechnology* **1**: 784–791.
421 Veith PD, Talbo GH, Slakeski N, Dashper SG, Moore C, Paolini RA & Reynolds EC
422 (2002) Major outer membrane proteins and proteolytic processing of RgpA and Kgp
423 of *Porphyromonas gingivalis* W50. *Biochem J* **363**: 105-115.
424 Yamaguchi M, Sato K, Yukitake H, Noiri Y, Ebisu S & Nakayama K (2010) A
425 *Porphyromonas gingivalis* mutant defective in a putative glycosyltransferase exhibits
426 defective biosynthesis of the polysaccharide portions of lipopolysaccharide,
427 decreased gingipain activities, strong autoaggregation, and increased biofilm
428 formation. *Infect Immun* **78**: 3801–3812.
429 Yang HW, Huang YF & Chou MY (2004) Occurrence of *Porphyromonas gingivalis*
430 and Tannerella forsythensis in periodontally diseased and healthy subjects. *J*
431 *Periodontol* **75**: 1077–1083.
432
433

434 **Figure Legends**

435

436 **Figure 1.** Immunoblot analysis with various *P. gingivalis* strains using anti-PepK.
437 Whole cell lysates of *P. gingivalis* wild-type strains, including the naturally
438 non-pigmented strain HG66 (a), T9SS-deficient mutants and the *pepK* mutant (b) and
439 A-LPS-deficient mutants (c) were subjected to immunoblot analysis with
440 anti-PGN_1416 (PepK).

441

442 **Figure 2.** Subcellular location of the PepK protein using immunoblot analysis. (a)
443 Whole cell lysates (W) of *P. gingivalis* ATCC 33277 were fractionated to the
444 cytoplasmic/periplasmic fraction (C/P) and the total membrane fraction (TM). (b) The
445 total membrane fraction was then fractionated by sucrose gradient centrifugation
446 resulting in the inner (IM) and outer (OM) membrane fractions. (c) The culture
447 supernatant (sup) was separated into the vesicle fraction (v.f.) and the particle-free
448 culture supernatant (p.f.f) by centrifugation. (d) Whole cells of *P. gingivalis* ATCC
449 33277 (WT), KDP355 (*porK*), KDP117 (*porT*) and KDP600 (*pepK*) were blotted
450 directly onto a nitrocellulose membrane. The blotted membrane was subjected to
451 immunodetection with anti-PepK or anti-PtpA. PtpA is a surface protein secreted
452 independently of T9SS.

453

454 **Figure 3.** Endopeptidase activity of the outer membrane fraction. The endopeptidase
455 activities of the outer membrane fractions of bacterial cells were determined with the
456 synthetic substrates Boc-Val-Leu-Lys-MCA (a) and Boc-Phe-Ser-Arg-MCA (b). Bar: 1,
457 KDP129 (*kgp*); 2, KDP601 (*kgp pepK*). (c) Cells of KDP601 (*kgp pepK*) and KDP981

458 (*kgp rgpA rgpB*) were inoculated into the same culture medium and incubated overnight
459 (co-culture). The endopeptidase activities of the outer membrane fractions of bacterial
460 cells were determined with Boc-Val-Leu-Lys-MCA. Bar: 1, KDP129 (*kgp*); 2, KDP601
461 (*kgp pepK*); 3, KDP981 (*kgp rgpA rgpB*); 4, co-culture of KDP601 and KDP981.
462
463 **Figure 4.** Immunoblot analysis of *P. gingivalis* mutants with various combinations of
464 *kgp, rgpA* and *rgpB* using anti-PepK. (a) Whole cell lysates of KDP129 (*kgp*), KDP131
465 (*rgpA*), KDP132 (*rgpB*), KDP134 (*kgp rgpA*), KDP135 (*kgp rgpB*), KDP133 (*rgpA*
466 *rgpB*), KDP981 (*kgp rgpA rgpB*), KDP136 (*kgp rgpA rgpB*) and KDP600 (*pepK*) were
467 subjected to immunoblot analysis with anti-PepK. (b) Another blot with whole cell
468 lysates of KDP133 (*rgpA rgpB*), KDP981 (*kgp rgpA rgpB*) and KDP136 (*kgp rgpA*
469 *rgpB*) was subjected to increased exposure times, resulting in appearance of the diffuse
470 band in KDP133. (c) Whole cell lysates of co-cultures of KDP601 (*kgp pepK*) and
471 KDP981 (*kgp rgpA rgpB*), KDP601, KDP981 and ATCC 33277 were subjected to
472 immunoblot analysis with anti-PepK.
473
474 **Figure 5.** Amino acid sequence comparisons of PepK homologues. (a) The
475 N-terminal regions including the catalytic domains. *Acidovorax citrulli* AAC00-1:
476 Aave_4239, *Lysobacter* sp. IB-9374: BAC22111, *Parabacteroides distasonis* ATCC
477 8503: BDI_2829, *Porphyromonas gingivalis* ATCC 33277: PGN_1416, *Pseudomonas*
478 *aeruginosa* PA7: PSPA7_0919, *Tannerella forsythia* ATCC 43037: BFO_3286,
479 *Xanthomonas albilineans* GPE PC73: XALc_2516. Asterisks indicate the putative
480 serine protease catalytic triad. (b) The C-terminal 80 amino acids of PepK homologues
481 of *P. gingivalis*, *P. distasonis* and *T. forsythia*. The alignment was created using the

482 ClustalW and Boxshade programs hosted at the Swiss EMBnet web site

Fig.1

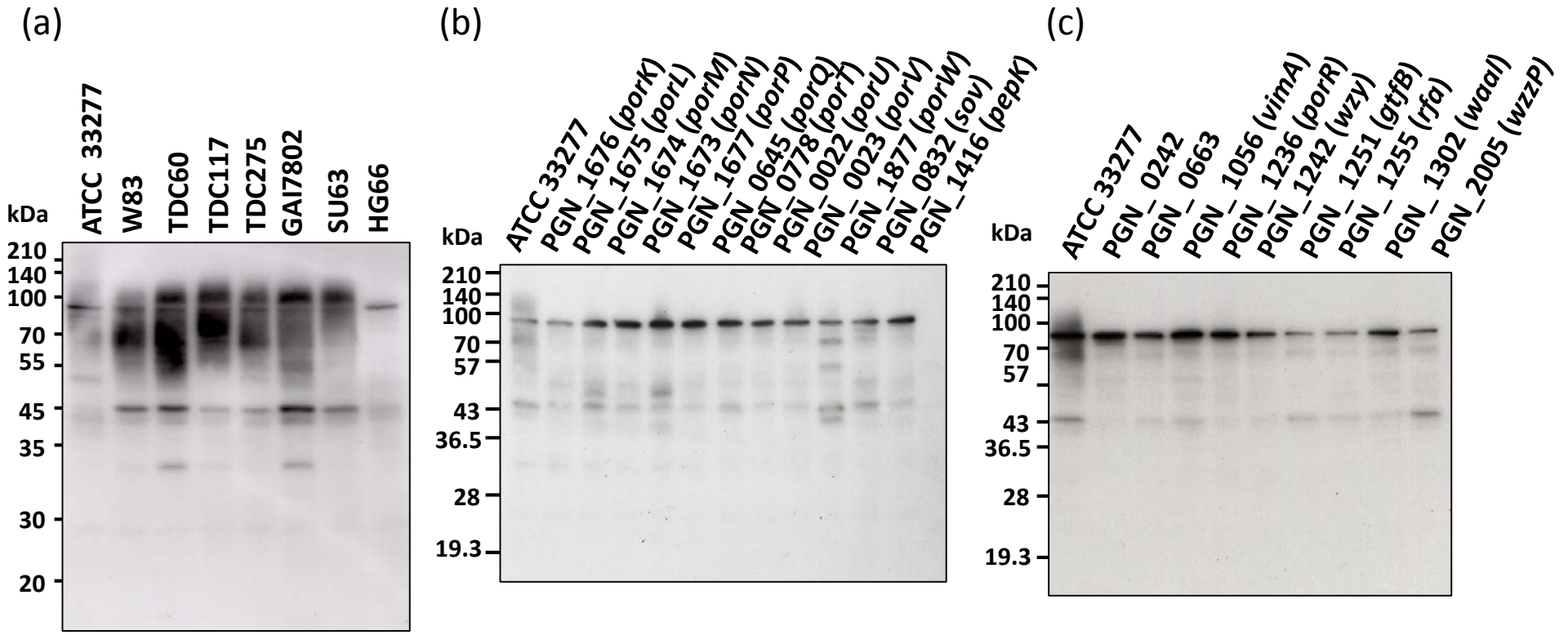
(a)
ATCC 33277
W83
TDC60
TDC117
TDC275
GAI7802
SU63
HG66
kDa
210
140
100
70
55
45
35
30
20
(b)
ATCC 33277
PGN_1676 (porK)
PGN_1675 (porL)
PGN_1674 (porM)
PGN_1673 (porN)
PGN_1677 (porP)
PGN_0645 (porQ)
PGN_0778 (porT)
PGN_0022 (porU)
PGN_0023 (porV)
PGN_1877 (porW)
PGN_0832 (sov)
PGN_1416 (pepK)
kDa
210
140
100
70
57
43
36.5
28
19.3
(c)
ATCC 33277
PGN_0242
PGN_0663
PGN_1056 (vimA)
PGN_1236 (porR)
PGN_1242 (wzy)
PGN_1251 (gtfB)
PGN_1255 (rfa)
PGN_1302 (waaI)
PGN_2005 (wzzP)
kDa
210
140
100
70
57
43
36.5
28
19.3

Fig.2

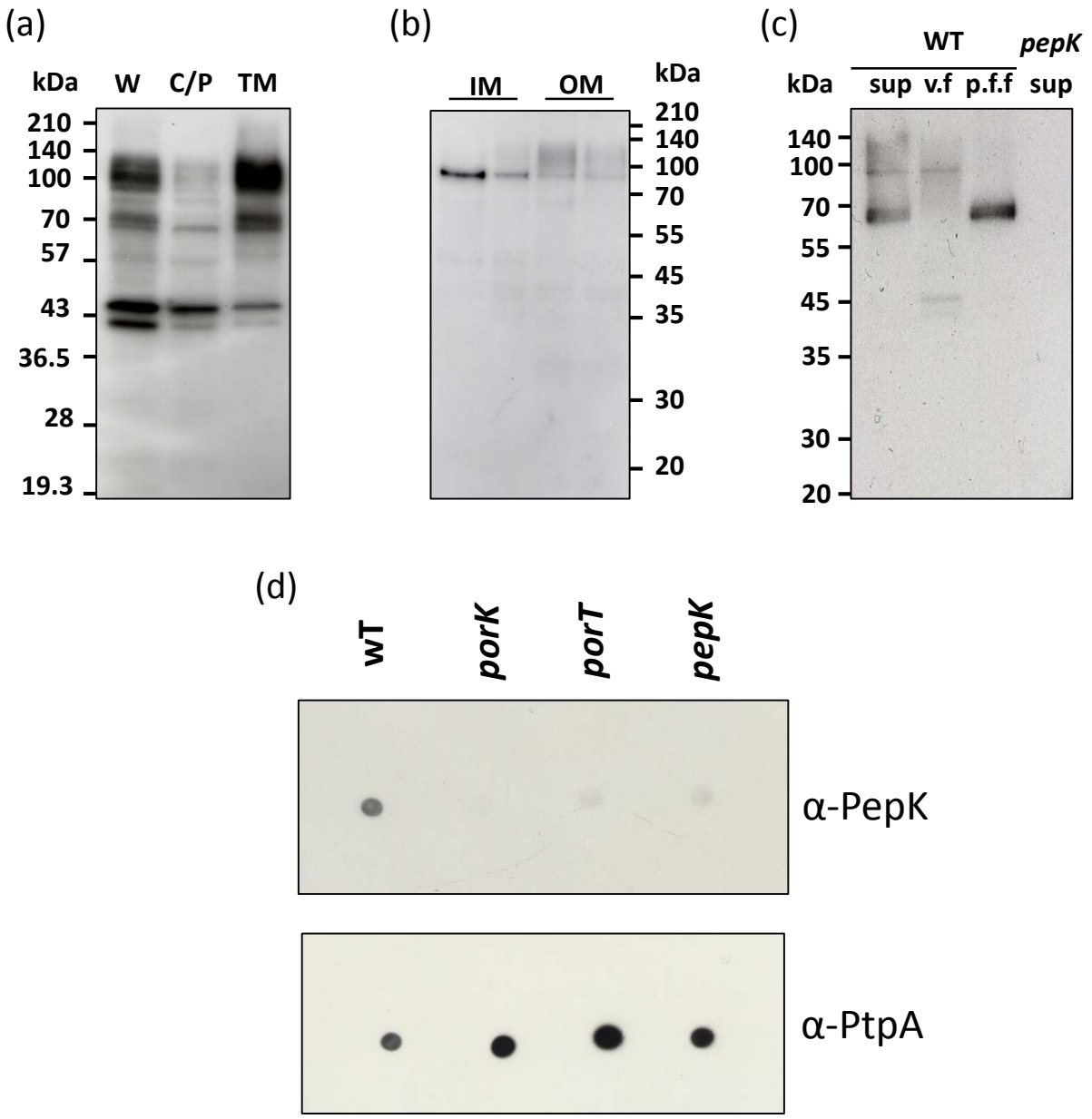
(a)
kDa
W
C/P
TM
210
140
100
70
57
43
36.5
28
19.3
(b)
IM
OM
kDa
210
140
100
70
55
45
35
30
20
(c)
WT
pepK
kDa
sup
v.f
p.f.f
sup
140
100
70
55
45
35
30
20
(d)
wT
porK
porT
pepK
α-PepK
α-PtpA

Fig.3

(a)

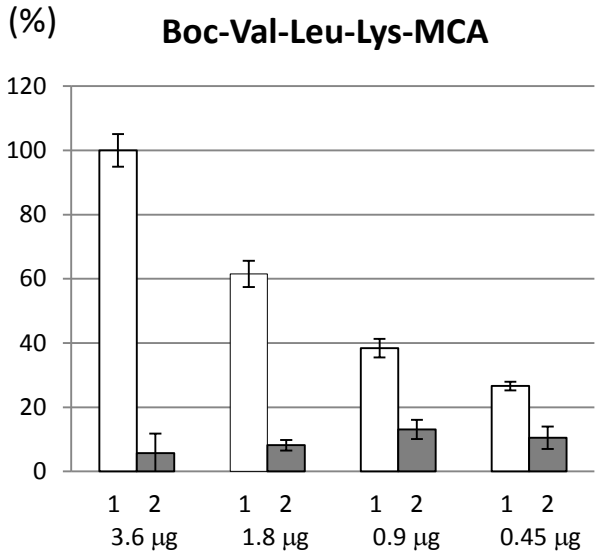
(%)
Boc-Val-Leu-Lys-MCA
120
100
80
60
40
20
0
1 2
3.6 μg
1 2
1.8 μg
1 2
0.9 μg
1 2
0.45 μg

(b)

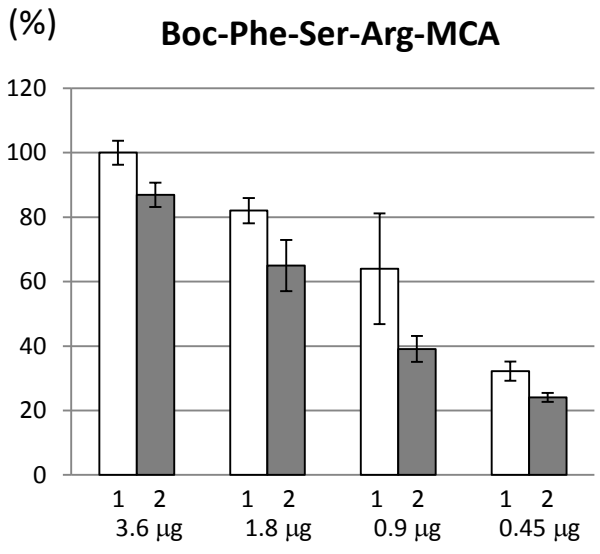
(%)
Boc-Phe-Ser-Arg-MCA
120
100
80
60
40
20
0
1 2
3.6 μg
1 2
1.8 μg
1 2
0.9 μg
1 2
0.45 μg

(c)

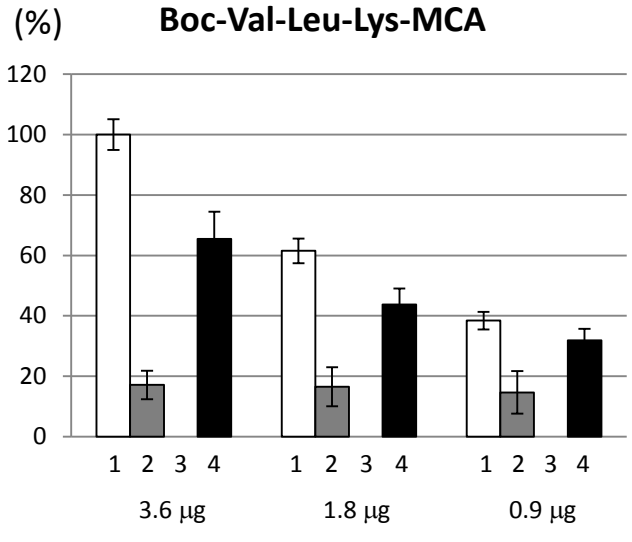
(%)
Boc-Val-Leu-Lys-MCA
120
100
80
60
40
20
0
1 2 3 4
3.6 μg
1 2 3 4
1.8 μg
1 2 3 4
0.9 μg

Fig.4

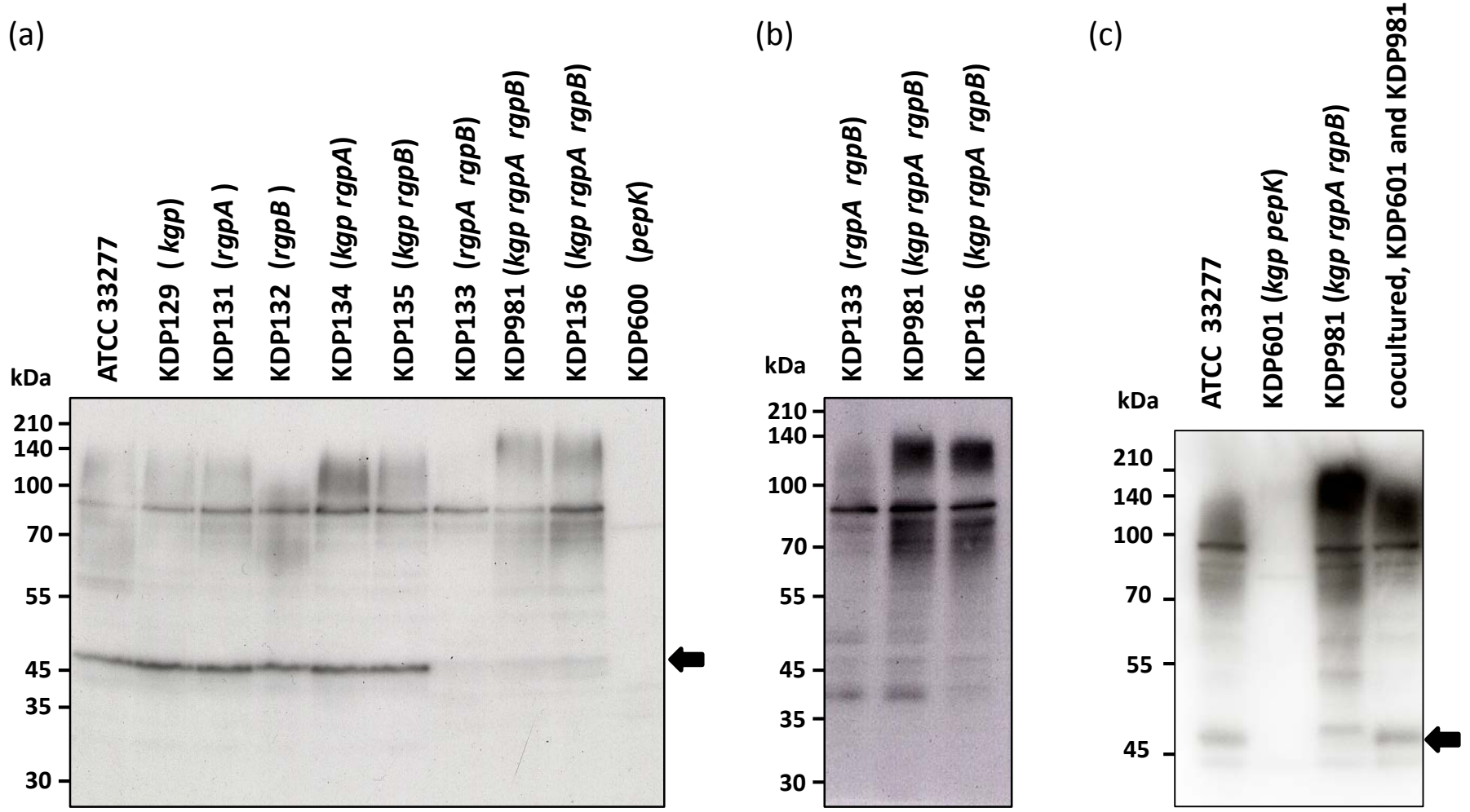
(a)
ATCC 33277
KDP129 (kgp)
KDP131 (rgpA)
KDP132 (rgpB)
KDP134 (kgp rgpA)
KDP135 (kgp rgpB)
KDP133 (rgpA rgpB)
KDP981 (kgp rgpA rgpB)
KDP136 (kgp rgpA rgpB)
KDP600 (pepK)
kDa
210
140
100
70
55
45
35
30
(b)
KDP133 (rgpA rgpB)
KDP981 (kgp rgpA rgpB)
KDP136 (kgp rgpA rgpB)
kDa
210
140
100
70
55
45
35
30
(c)
ATCC 33277
KDP601 (kgp pepK)
KDP981 (kgp rgpA rgpB)
cocultured, KDP601 and KDP981
kDa
210
140
100
70
55
45

Fig. 5

(a)

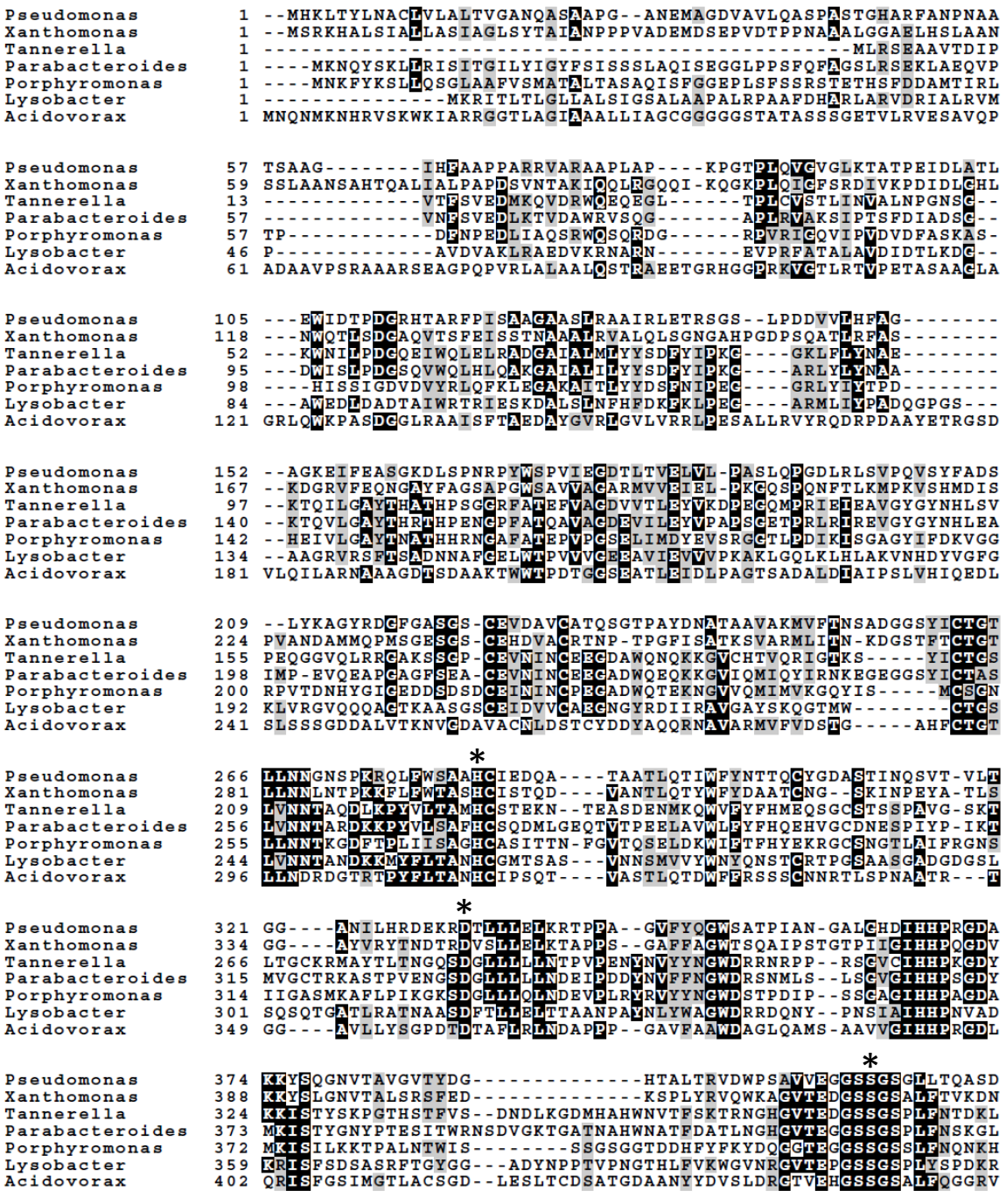
Pseudomonas
Xanthomonas
Tannerella
Parabacteroides
Porphyromonas
Lysobacter
Acidovorax

(b)

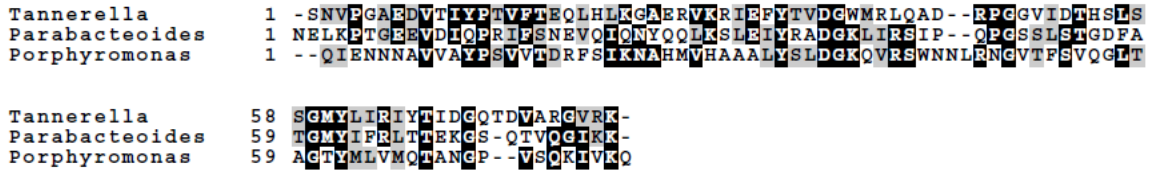
Tannerella
Parabacteoides
Porphyromonas

Table 1. Effects of proteinase inhibitors on Lys-specific endopeptidase activity.

Proteinase inhibitor	**Residual activity (%)**
TLCK	61.6
Leupeptin	0
Antipain	0
Chymostatin	53.9
Pepstatin	113.6
EDTA-Na_2	142.9
No inhibitor	100

Inhibitory effects of proteinase inhibitors on the Lys-specific endopeptidase were calculated using the following formula: (difference of the activities of KDP129 and KDP601 in the reaction mixture with inhibitors / difference of the activities of KDP129 and KDP601 in the reaction mixture without inhibitors) x 100 (%).